Prediction of Inlet Duct Overpressures Resulting from Engine Surge

Franklin L. Marshall*
The Boeing Company, Seattle, Wash.

A semiempirical method has been developed for predicting the peak surge-induced overpressures in the vicinity of the engine face as a function of engine cycle variables. The method is applicable to relatively long inlets, such as those typically used on supersonic airplanes. (For the shorter inlets typical of subsonic airplanes pressure relief is obtained at the inlet entrance before the peak overpressures are reached in the inlet.) A correlation of existing overpressure data is obtained by combining an analytical solution for the effect of engine bypass ratio with an empirical evaluation of the effect of over-all compressor pressure ratio. The resulting method can be used to obtain boundary conditions for inlet dynamic simulation programs that predict the effects of inlet duct geometry and auxiliary air systems on overpressure characteristics. The method predicts that higher engine bypass ratios lead to significant reductions in peak overpressures.

Nomenclature†

A = flow area
a = speed of sound
AR_{EFF} = effective area ratio
BPR = bypass ratio
K = overpressure parameter = $\Delta p/(p_1 M_1^{1.26})$
M = Mach number
p = pressure
u = velocity
T_t = total temperature
Δp = pressure rise due to the passage of an upstream-propagating shock wave
ξ = $A_{3U}/(A_{3U} + A_{3L})$
ρ = density

Introduction

KNOWLEDGE of inlet overpressure characteristics following engine surge is of fundamental importance to the designer of a supersonic inlet. Such inlets are generally of sufficient length that a surge-generated pressure pulse, often called a hammershock, peaks at a value considerably in excess of freestream stagnation pressure before relief is obtained at the entrance of the inlet. Peak hammershock pressures as much as 65 to 70% larger than freestream stagnation pressures have been observed in such an inlet.[1] Some subsonic inlets, such as the center-engine S-duct inlet of the 727 airplane, are also long enough to produce similar hammershock phenomena. For such inlets accurate estimates of the hammershock overpressures are essential for determining inlet structural requirements.

The hammershock appears to originate as a somewhat unsymmetrical disturbance. Experimenting with engine surges in a well instrumented J85-13 engine, Choby, Burstadt, and Calogeras[2] observed a stall zone as an "axial channel" extending through the compressor and rotating at one-half rotor speed. Its size expanded circumferentially as it rotated until it included the entire compressor after about three to four rotor rotations. Using another J85-13 engine, Sussman, Lampard, et al.,[3] found that the hammershock wave had not yet formed a one-dimensional plane wave when it propagated into the inlet upstream of the compressor. Measuring peak pressures at five circumferential and radial positions just upstream of the compressor face, they found that the highest peak pressure observed exceeded the lowest peak by about 15% of the average value.

Although this lack of symmetry can create additional problems in fixing inlet structural requirements, the primary problem facing the inlet structural designer remains the prediction of the maximum over-all pressure level reached in the inlet. The present paper is directed towards the solution of this latter problem.

Evidence can readily be found in the histories of recent airplane development programs that an adequate solution has not yet been found. The inlet on the F107A airplane sustained major structural damage during flight test as a result of an engine surge.[4] A similar incident, which occurred during engine surge tests in the Concorde flight test program,[5] forced the temporary grounding of that aircraft for inlet structural modifications.

Past analytical studies of the hammershock phenomenon have generally involved dynamic simulation models of the inlet flowfield, such as the numerical finite-difference program developed by Mays.[6] Such programs are ideal for evaluating the effects of inlet duct geometry and auxiliary air or bleed systems on hammershock flowfields within an inlet. For an accurate solution, however, they require as boundary conditions the exact flow history at the compressor face during surge, and this, in Mays' words, is a "most elusive quantity."

Past attempts to obtain empirical correlations of hammershock overpressure data have concentrated on the surge characteristics of a single engine. Bellman and Hughes[7] obtained an excellent correlation of surge data for the TF-30 engine resulting from NASA's F111A flight test program. They showed that the maximum hammershock pressure was nearly a constant fraction of the compressor discharge pressure, ranging from 14% at low compressor pressure ratios to 12% at high compressor pressure ratios. This result was valid over a wide range of altitudes and Mach numbers. Choby, Burstadt, and Calogeras observed a similar correlation with data from their J85-13

Received November 15, 1972; presented as Paper 72-1142 at the AIAA/SAE 8th Joint Propulsion Specialist Conference, New Orleans, La., November 29–December 1, 1972; revision received March 7, 1973. The author would like to thank G. W. N. Lampard, who first suggested the application of the solution of the original problem (illustrated in Fig. 2) to the present problem. Thanks also are due J. P. Zeeben, who was able to locate sufficient engine performance data to infer presurge compressor face Mach numbers when such information was not directly available from existing hammershock data.

Index categories: Subsonic and Supersonic Airbreathing Propulsion; Aircraft Structural Design (Including Loads).

*Specialist Engineer. Member AIAA.

† The subscripts 1, 2, 3, 3U, 3L, 3M, 4, and S, indicate different regions of the flowfield studied, and are identified in Fig. 4.

test program, but the peak pressures were a much higher fraction (25 to 30%) of the compressor discharge pressure.

A semiempirical method for predicting these hammer-shock overpressures in the vicinity of the engine face is offered here. The primary goal is to account for the effect of engine cycle variables, specifically bypass ratio and compressor pressure ratio.

Approach

A solution originally obtained by the author for surge-induced flow phenomena in a bifurcated inlet duct feeding two engines is applied to the present problem. The original solution predicted the effect of a surge of one engine on an adjacent engine. The engines were separated by a moderately long splitter plate. The analysis assumed the flowfield evolution shown in Fig. 1. The emergence of a surge-generated shock wave from behind the splitter plate was assumed to result ultimately in a downstream-propagating shock wave approaching the operating engine, an upstream-propagating shock wave in the main inlet duct, and a reflected expansion wave approaching the surging engine.

The application to the present problem is based on the analogy, illustrated in Fig. 2, between the original flow geometry and that of the front part of a turbofan engine. The duct of the surging engine is now considered analogous to the core flow duct of the turbofan engine. The emphasis of the original problem was on predicting the strength of the shock transmitted down the duct of the operating engine, analogous now to the fan duct. The emphasis here is on the strength of the shock transmitted upstream in the inlet duct.

In applying the original solution, the surge flow phenomenon is modeled as follows:

1) A high-amplitude surge originates with the stalling of the core compressor. This is considered similar to the rupturing of the diaphragm in a shock tube, with the high pressure compressor discharge air corresponding to the driver gas. The resulting compression waves do not immediately take the form of a fully coalesced shock wave, of course, nor do they form one-dimensional plane waves, as noted earlier. However, they are treated as a plane shock wave so that the resulting fan duct interactions can be readily analyzed to a reasonable degree of approximation.

2) The strength of the surge, as measured by the drop in core compressor airflow, is a function of the presurge compressor pressure ratio only. It is specifically independent of engine bypass ratio.

3) The fan duct provides extra area into which high pressure air may flow, thereby reducing the inlet duct overpressures.

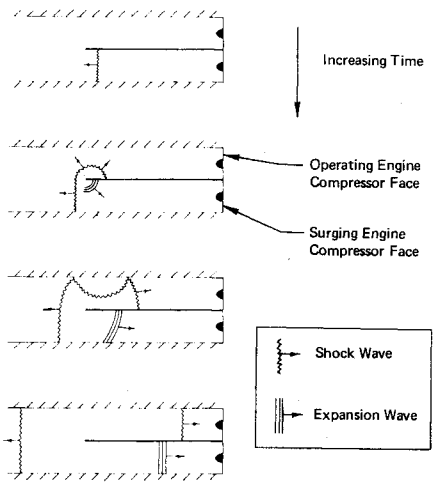

Fig. 1 Assumed flowfield evolution.

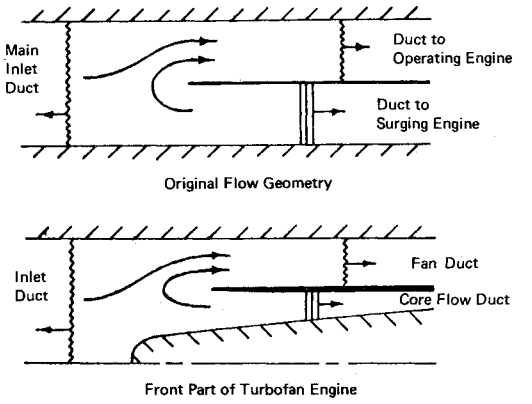

Fig. 2 Analogy behind application to present problem.

Solution of Original Problem

Three types of solutions were identified, as illustrated in Fig. 3. The Type 1 solution involves no reverse flow in any of the ducts. For Type 2 solutions the initial incident shock wave is strong enough to reverse the flow (or slow the flow enough that the reflected expansion wave causes reverse flow), but the shock wave transmitted into the main inlet duct does not reverse the flow direction. In the Type 3 solutions, both the incident and transmitted shock waves are strong enough to produce reverse flow in their respective ducts. Only Type 2 solutions were sought, since they cover most of the range of interest, and, as will be shown, Type 1 solutions can be inferred from the Type 2 solutions.

For a brief time following the emergence of the incident shock wave, considerable reflection of acoustic waves occurs between the region of the end of the splitter plate and the outward-propagating waves. Following this period, however, the flow is assumed to reach a quasi-equilibrium condition for which steady-state conditions prevail in the region of the end of the splitter plate, and plane shock waves or expansion waves are propagating away from this region in the three flow ducts.

The resulting flowfield is sketched in Fig. 4, which also identifies the different flow regions involved. There are six regions, labeled 2, 3U, 3L, 3M, 3, and 4, in which conditions are unknown. The complete definition of conditions in each region requires knowledge of three variables: two state variables, such as pressure p and density ρ (a perfect gas has been assumed), and one flow variable, such as velocity u or mass flux ρu. The relative size of the flow areas

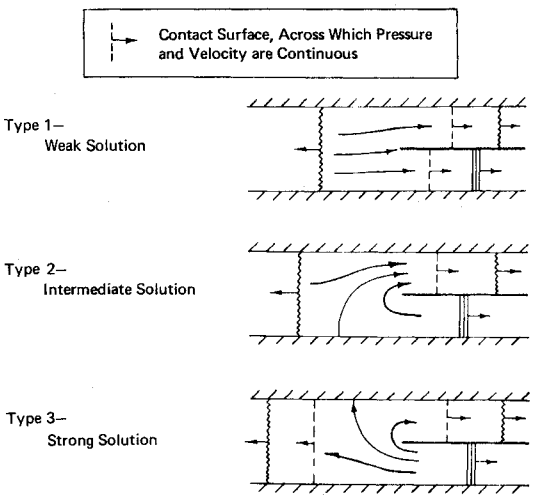

Fig. 3 Three types of solutions.

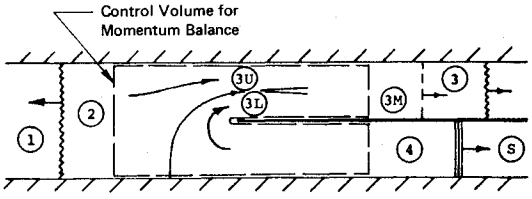

Fig. 4 Key flow regions.

for region 3U and 3L, given by the fraction

$$\xi = A_{3U}/(A_{3U} + A_{3L})$$

is also unknown. Thus there are essentially 19 unknowns. The initial undisturbed conditions in region 1, and the strength of the incident shock wave, and thus conditions in region S, are known at the outset.

Two of the required 19 relations result from specifying the relative flow areas involved. Thus the area ratio A_3/A_S is specified, and A_2 must equal the sum of A_3 and A_S. The other 17 relations result from satisfying the following conditions:

1) Conditions in regions 2 and 3 result from the passage of shock waves in the appropriate directions. This effectively provides two of the three relations necessary to determine conditions in each of these regions. If some measure of shock strength were also known, conditions behind the shock wave would then be uniquely determined. (An example of the relationships implied by this condition is given in Fig. 5, which relates the pressure ratio across the transmitted shock to the mass flux drop produced in region 2 as a function of initial duct Mach number. This figure, often useful in dealing with upstream-propagating shock waves, will be discussed further in the following section.)

2) Conditions in region 4 result from the downstream propagation of an expansion wave into region S. This too provides two of the three relations required to determine conditions behind the wave. Only the over-all strength of the expansion wave remains to be determined.

3) The streamtubes from regions 2 and 4 can merge subsonically at equal pressure into the streamtubes in regions 3U and 3L, respectively. In addition to the pressure equality, this implies equality of mass flow rates between regions 2 and 3U, and between regions 4 and 3L. In each case it is also assumed that the transition into the new streamtubes occurs isentropically.

4) Complete mixing of the 3U and 3L streamtubes to uniform conditions produces the 3M streamtube, having the same pressure and velocity as the streamtube of region 3. The result of mixing the 3U and 3L streamtubes is calculated with the appropriate conservation equations for mass, momentum, and energy:

$$(\rho u)_{3U}\xi + (\rho u)_{3L}(1-\xi) = (\rho u)_{3M}$$

$$(p + \rho u^2)_{3U}\xi + (p + \rho u^2)_{3L}(1-\xi) = (p + \rho u^2)_{3M}$$

$$(\rho u)_{3U}\xi T_{t_{3U}} + (\rho u)_{3L}(1-\xi)T_{t_{3L}} = (\rho u)_{3M}T_{t_{3M}}$$

The subsonic solution for conditions in region 3M is used, of course, in deference to the second law.

5) The steady-state momentum equation is satisfied in the region of the end of the splitter plate. Thus, using the control volume shown in Fig. 4, the required condition is:

$$(p + \rho u^2)_2 A_2 = (p + \rho u^2)_4 A_S + (p + \rho u^2)_{3M} A_3$$

Simultaneous solutions of the preceding relations have been obtained through the use of an iterative technique with the CDC 6600 computer. The solutions for the strength of the shock wave transmitted upstream are given in Fig. 6. Type 1 solutions, shown as dashed lines, represent interpolations between Type 2 solutions and the trivial Type 1 solution given by mass flux ratios of unity for both incident and transmitted shock waves (corresponding to no disturbance). Mass flux ratios have been used to specify shock strength because the resulting solutions are quite

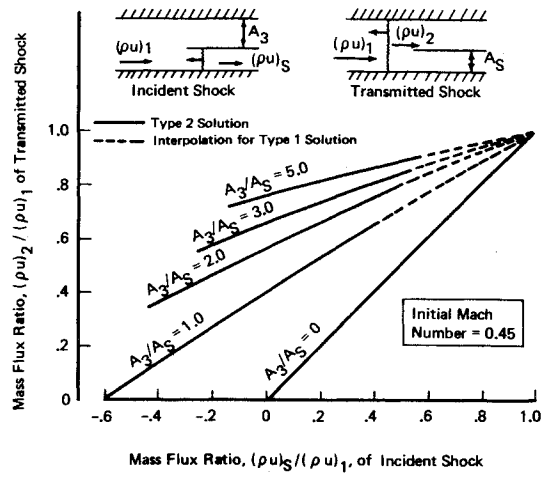

Fig. 6 Solutions to original problem.

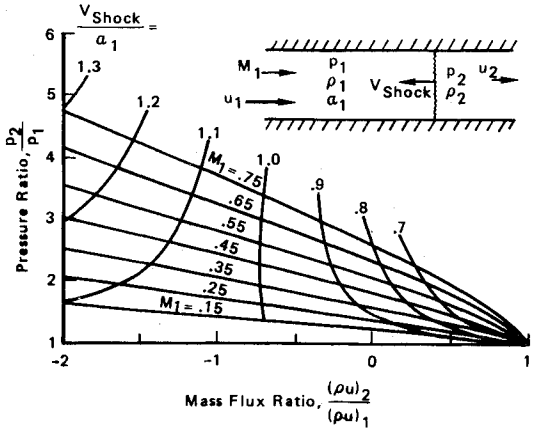

Fig. 5 Pressure/mass-flow relationships for an upstream-propagating shock wave.

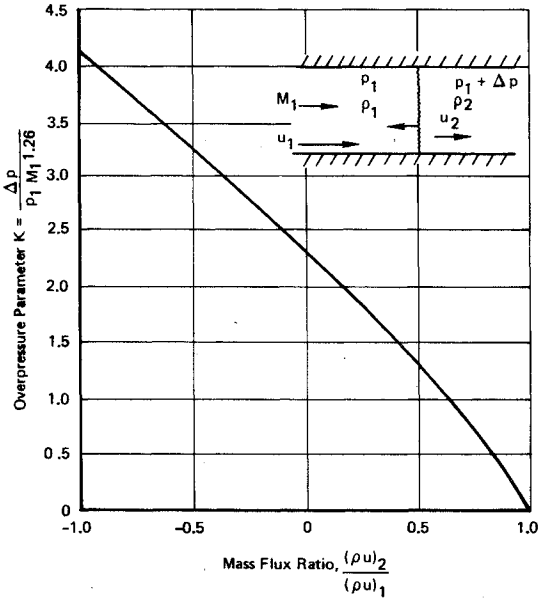

Fig. 7 Approximate pressure/mass-flow relationship for an upstream-propagating shock wave.

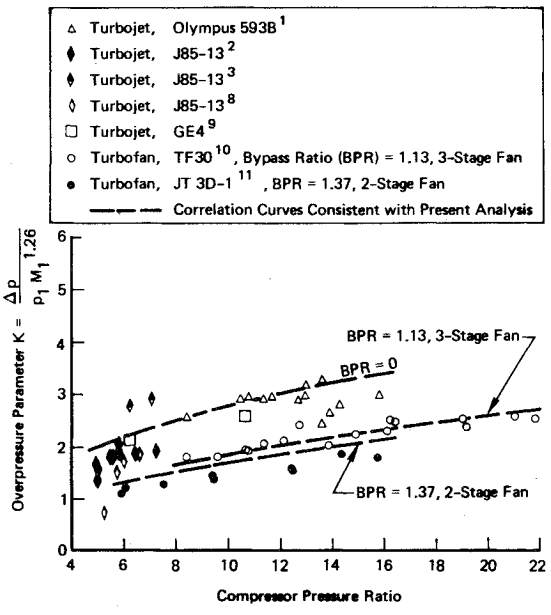

Fig. 8 Correlation curves and supporting data.

insensitive to initial Mach number over the range of Mach numbers of interest.

The range of solutions is limited at the lower transmitted-shock mass flux ratios (corresponding to stronger shocks) by one of two constraints. At the higher values of the area ratio A_3/A_S the strength of the reflected expansion wave causes the flow in region 4 to approach sonic conditions as the shock strengths are increased. This results in the breakdown of the assumption of isentropic subsonic flow between region 4 and 3L. At low area ratios (e.g., an area ratio of 1.0) the limiting condition for Type 2 solutions, i.e., a transmitted-shock mass flux ratio of zero, is reached.

Application to Present Problem

The effective mass flux ratio of the initial shock wave generated within the core flow of a surging turbofan engine was assumed to be a unique function of pre-surge over-all compressor pressure ratio. The effect of the fan duct in attenuating the shock transmitted into the inlet duct was then found from Fig. 6. The effective ratio of fan duct area to core flow area was initially taken to be the nominal sea-level static bypass ratio of the engine. The relationship between initial shock mass flux ratio and compressor pressure ratio was then adjusted to give the best fit to available hammershock data. The agreement with the data was found to improve when the blockage due to the fan stages was assumed to reduce the effective fan duct area by 5% for each fan stage.

Use has also been made of an approximation to the hammershock relationships given in Fig. 5. It can be shown that for a given mass flux ratio the percentage increase in pressure is approximately proportional to the initial Mach number to the 1.26 power. Thus the curves of Fig. 5 can be reduced to a single curve by defining an overpressure parameter K:

Insei $$K = \Delta p/(p_1 M_1^{1.26})$$

where $\Delta p/p_1$ is the fractional pressure increase. The resulting curve, shown in Fig. 7, is accurate to within about 5% over a range of parameters of practical interest. For the convenience of the user, the correlation of the inlet duct overpressures has been obtained in terms of the parameter K, rather than mass flux ratio.

The correlation curves, as well as the supporting data, are given in Fig. 8. The empirically derived relationship

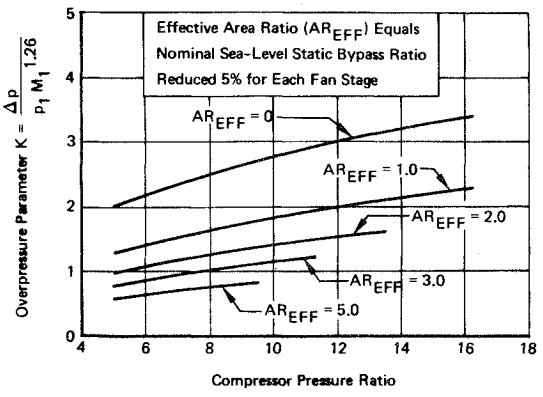

Fig. 9 Predicted hammershock overpressures.

between initial shock mass flux ratio and compressor pressure ratio is in effect given by the curve for bypass ratio zero, since this curve allows for no attenuation. The other curves can be analytically derived from this bypass-ratio-zero curve by appropriate application of the results given in Fig. 6.

All of the data in the figure represent peak pressures observed in the inlet duct in the immediate vicinity of the engine face, usually just upstream of the engine spinner. The Mach numbers used in defining K represent a corresponding inlet station, just upstream of the spinner. Some of the data[3,10] represent the average of the peak pressures obtained at several circumferential and radial locations, but most represent measurements at a single location. In view of the nonsymmetrical effects noted earlier, this probably accounts for some of the scatter in the data. Nevertheless, the correlation curves account for all of the data, except an occasional low point, within 9% of the absolute hammershock pressure level. In the case of each of the very low data points, other data for the same engine at virtually the same operating conditions show that higher overpressures are possible.

Figure 9 presents a more general form of the correlation, including predictions for higher area ratios based on the procedures described above. The range of predictions for the higher area ratios does not extend to high pressure ratios because of the previously described limits to the range of solutions in Fig. 6.

Conclusions

A semiempirical correlation method has been found for predicting peak inlet duct overpressures near the engine face resulting from engine surge. The method is applicable to relatively long inlet ducts, such as those typically used on supersonic airplanes. The underlying theoretical basis allows predictions for engines of higher bypass ratios than those for which hammershock data are currently available. Increasing bypass ratios are predicted to cause significant reductions in peak overpressures. The results can also be used to help generate the boundary conditions for inlet dynamic simulation programs which predict the effect of duct geometry and auxiliary air or bleed systems on hammershock characteristics. Future work could profitably be directed toward extending the range of predictions to higher compressor pressure ratios.

References

[1]Morris, D. P. and Williams, D. D., "Free-Jet Testing of A Supersonic Engine/Intake Combination," *The Aeronautical Journal of the Royal Aeronautical Society*, Vol. 74, March 1970, pp. 212–218.

[2]Choby, D. A., Burstadt, P. L., and Calogeras, J. E., "Unstart and Stall Interactions between a Turbojet Engine and an Axi-

symmetric Inlet with 60-Percent Internal-Area Contraction," TM X-2192, March 1971, NASA.

[3]Sussman, M. B., Lampard, G. W. N., et al., "A Study of Inlet/Engine Interaction in a Transonic Propulsion Wind Tunnel," D6-60116, Jan. 1970, The Boeing Co., Seattle, Wash.

[4]Randall, L. M. and Hand, W. H., "Integration of Inlet and Engine—Airplane Man's Point of View," NA 68-136, 1968, North American Rockwell Corp., Los Angeles, Calif.

[5]Williams, D. D., Private communication, Jan. 1973, Bristol Engine Division, Rolls-Royce Ltd. (1971), Bristol, England.

[6]Mays, R. A., "Inlet Dynamics and Compressor Surge," *Journal of Aircraft*, Vol. 8, No. 4, April 1971, pp. 219–226.

[7]Bellman, D. R. and Hughes, D. L., "The Flight Investigation of Pressure Phenomena in the Air Intake of an F-111A Airplane," AIAA Paper 69-488, Colorado Springs, Colo., 1969.

[8]Mitchell, G. A. and Johnson, D. F., "Experimental Investigation of the Interaction of a Nacelle-Mounted Supersonic Propulsion System with a Wing Boundary Layer," TM X-2184, March 1971, NASA.

[9]SST Coordination Memo, TM 69-496, July 16, 1969, The General Electric Co., Evendale, Ohio.

[10]Nugent, J., Private communication, Aug. 1972, NASA Flight Research Center, Edwards, Calif.

[11]Unpublished data, Boeing Co., Seattle, Wash.

MAY 1973 J. AIRCRAFT VOL. 10, NO. 5

Advanced Supersonic Inlet Technology

Norman E. Sorensen,* Donald B. Smeltzer,† and Eldon A. Latham†
NASA Ames Research Center, Moffett Field, Calif.

Recently, relatively new analytical procedures have been successfully used to design bleed systems for mixed-compression inlets designed to operate efficiently up to Mach number 2.65. The procedures used constitute a major advance in inlet technology by offering a promising approach to attain high internal and external performance for mixed-compression inlets that operate over a large supersonic Mach number range. Unfortunately, there is a lack of data describing bleed hole performance characteristics to verify these procedures at high Mach numbers. Further, as the Mach number increases, inlets with bleed systems become more difficult to design because the available methods do not properly account for the boundary-layer growth in large adverse pressure gradients, particularly in shock-wave impingement regions. Also, regardless of the analytical methods available, the design of bleed systems that can operate efficiently over wide Mach number ranges is a challenging problem because it is difficult to satisfy both cruise and off-design bleed requirements. This paper briefly discusses the analytical procedures for designing advanced inlet systems and suggests facility modifications wherein the procedures can be verified on large-scale inlet models up to approximately Mach number 4.5.

Nomenclature

A_c = capture area
d = hole diameter
h = throat height
l = hole length
M = Mach number
$\bar{M}_L$ = average local Mach number
m = mass flow
m_∞ = capture mass flow, $\rho_\infty U_\infty A_c$
N = boundary-layer power-law exponent
p = static pressure
p_p = pitot pressure
p_t = total pressure
$\bar{p}_t$ = area-weighted average total pressure
p_{p_l} = plenum chamber pressure
Δp = pressure rise to throat of inlet
R = cowl lip radius
U = velocity
x = axial station measured from tip of centerbody
α = angle of attack
β = angle of sideslip
δ^* = boundary-layer displacement height
η_{KE} = kinetic energy efficiency
ρ = density

Subscripts

b_l = bleed
DES = design
L = local
e = freestream exit
2 = engine face
δ = boundary-layer edge
∞ = freestream

Received December 4, 1972; revision received February 26, 1973.
Index category: Subsonic and Supersonic Airbreathing Propulsion.

* Research Scientist, Aerodynamics Branch. Member AIAA.
† Research Scientist, Aerodynamics Branch.

Introduction

MANY aircraft have been developed that operate efficiently up to approximately Mach number 2.5. Between Mach number 2.5 and 3.5, only a few aircraft have been developed and beyond Mach number 3.5, virtually none. Propulsion research for such aircraft have, unfortunately, followed a similar pattern; i.e., little effort has been placed on analytical and experimental research in the Mach number range above 2.5. As a result, the technology for the design of efficient inlet systems for aircraft flying below Mach number 2.5 is well developed. Conversely, in the higher supersonic range (from approximately $M = 3.0$ to 4.5), current technology does not adequately account for such phenomena as high adverse pressure gradients, severe shock-wave boundary-layer interactions, and the greater Mach number range over which the inlet systems must operate efficiently. However, it appears from recent studies that the required technology can be developed. This paper will show the trend of advanced supersonic inlet technology and some of the important analytical and ex-